J|A|C|S
ARTICLES
Published on Web 06/23/2006

Sensitization of Cancer Cells to DNA Damaging Agents by Imidazolines

Vasudha Sharma, Satyamaheshwar Peddibhotla, and Jetze J. Tepe*

Contribution from the Department of Chemistry, Michigan State University, East Lansing, Michigan 48824

Received March 2, 2006; E-mail: tepe@chemistry.msu.edu

Abstract: Apoptosis, or programmed cell death, is a cellular mechanism used to regulate cell number and eliminate damaged or mutated cells. Concomitant with the initiation of the apoptotic cell signal, chemotherapeutic agents also induce anti-apoptotic factors, such as NF-κB, which compromise the overall efficacy of chemotherapeutic anticancer treatment. Here we describe an adjuvant therapy in which a small molecule is used to sensitize cancer cells toward apoptosis induced by chemotherapeutics. Our results indicate that the imidazoline **1d** modulates the pro-survival NF-κB pathway and selectively sensitizes cancer cells toward DNA damaging agents, thus enhancing the overall efficacy of the treatment. Pretreatment of cancer cells with the noncytotoxic imidazoline **1d** (10 nM) resulted in a significant increase in apoptosis and anticancer efficacy of the clinically significant DNA damaging agents camptothecin and cisplatin. Noncancerous cells remained unaffected during this regimen.

Introduction

Apoptosis (or programmed cell death) is a sequential, stepwise defensive mechanism to remove infected, mutated, or damaged cells.[1] Conventional anticancer therapy involving chemotherapy or ionizing radiation is aimed at the induction of apoptosis in cancer cells.[2] Camptothecin (CPT) is a plant alkaloid that exhibits specificity for DNA topoisomerase I and induces a stable ternary topoisomerase I−DNA cleavable complex.[3,4] Stabilization of this cleaved DNA complex is recognized as damaged DNA and initiates an apoptotic signaling pathway, culminating in cell death.[4,5] The clinically used DNA damaging agent, cisplatin (CDDP), exerts its anticancer activity via the covalent binding to DNA base pairs, which triggers a similar apoptotic signaling pathway.[6] In response to this drug-induced DNA assault, a range of signaling cascades involved in apoptosis, cell cycle arrest, and DNA repair are activated. This is tightly controlled by several regulatory pathways, including the pro-apoptotic p53 and the pro-survival NF-κB pathways.[7,8] Unfortunately, due to mutations that interfere with drug-induced initiation or execution of apoptosis, the pro-apoptotic response is abnormally down-regulated and provides an intrinsic survival advantage in many types of cancers.[9] Additional cellular resistance has been attributed to the activation of anti-apoptotic signaling pathways such as EGFR and NF-κB, which are induced after CPT treatment.[10,11] Strategies using combinations of inducers of apoptosis and/or inhibitors of anti-apoptotic factors with traditional chemotherapeutic drugs may therefore provide an improved alternative to conventional chemotherapy.[12−14] Hence, the search for new chemotherapeutic strategies has therefore shifted to small molecules that can selectively induce apoptosis in cancer cells or retard the cellular chemoresistance.[15,16]

(1) (a) Hengartner, M. O. *Nature* **2000**, *407*, 770−776. (b) Thompson, C. B. *Science* **1995**, *267*, 1456−1462.
(2) Schmitt, C. A.; Lowe, S. W. *J. Pathol.* **1999**, *187*, 127−137.
(3) (a) Hertzberg, R. P.; Caranfa, M. J.; Hecht, S. M. *Biochemistry* **1989**, *28*, 4629−4638. (b) Thomas, C. J.; Rahier, N. J.; Hecht, S. M. *Bioorg. Med. Chem.* **2004**, *12*, 1585−1604. (c) Pourquier, P.; Pommier, Y. *Adv. Cancer Res.* **2001**, *80*, 189−216.
(4) Pommier, Y.; Pourquier, P.; Fan, Y.; Strumberg, D. *Biochim. Biophys. Acta* **1998**, *1400*, 83−105.
(5) Macdonald, T. L.; Labroli, M. A.; Tepe, J. J. DNA topoisomerase II inhibitors. In *Comprehensive natural products chemistry*; Elsevier-North Holland: Amsterdam, 1999; pp 593−614.
(6) (a) Cohen, S. M.; Lippard, S. J. *Prog. Nucleic Acid Res. Mol. Biol.* **2001**, *67*, 93−130. (b) Wang, D.; Lippard, S. J. *Nat. Rev. Drug Discovery* **2005**, *4*, 307−320. (c) Jamieson, E. R.; Lippard, S. J. *Chem. Rev.* **1999**, *99*, 2467−2498. (d) Barnes, K. R.; Lippard, S. J. *Met. Ions Biol. Syst.* **2004**, *42*, 143−177. (e) Sedletska, Y.; Giraud-Panis, M. J.; Malinge, J. M. *Curr. Med. Chem.: Anti-Cancer Agents* **2005**, *5*, 251−265.
(7) (a) Boland, M. P. *Biochem. Soc. Trans.* **2001**, *29*, 674−678. (b) Maldonado, V.; Melendez-Zajgla, J.; Ortega, A. *Mutat. Res.* **1997**, *381*, 67−75. (c) Meek, D. W. *DNA Repair* **2004**, *3*, 1049−1056. (d) Karin, M.; Lin, A. *Nat. Immunol.* **2002**, *3*, 221−227. (e) Zhou, B. B.; Elledge, S. J. *Nature* **2000**, *408*, 433−439.
(8) Luo, J. L.; Kamata, H.; Karin, M. *J. Clin. Invest.* **2005**, *115*, 2625−2632.
(9) Johnstone, R. W.; Ruefli, A. A.; Lowe, S. W. *Cell* **2002**, *108*, 153−164.
(10) (a) Wang, C. Y.; Mayo, M. W.; Korneluk, R. G.; Goeddel, D. V.; Baldwin, A. S., Jr. *Science* **1998**, *281*, 1680−1683. (b) Carson, J. P.; Zhang, N.; Frampton, G. M.; Gerry, N. P.; Lenburg, M. E.; Christman, M. F. *Cancer Res.* **2004**, *64*, 2096−2104. (c) Pomerantz, J. L.; Baltimore, D. *Nature* **2000**, *406*, 26−29.
(11) Cusack, J. C.; Liu, R.; Baldwin, A. S. *Drug Resist. Updates* **1999**, *2*, 271−273.
(12) Vaziri, S. A.; Hill, J.; Chikamori, K.; Grabowski, D. R.; Takigawa, N.; Chawla-Sarkar, M.; Rybicki, L. R.; Gudkov, A. V.; Mekhail, T.; Bukowski, R. M.; Ganapathi, M. K.; Ganapathi, R. *Mol. Cancer Ther.* **2005**, *4*, 1880−1890.
(13) Mitsiades, N.; Mitsiades, C. S.; Richardson, P. G.; Poulaki, V.; Tai, Y. T.; Chauhan, D.; Fanourakis, G.; Gu, X.; Bailey, C.; Joseph, M.; Libermann, T. A.; Schlossman, R.; Munshi, N. C.; Hideshima, T.; Anderson, K. C. *Blood* **2003**, *101*, 2377−2380.
(14) Hideshima, T.; Chauhan, D.; Richardson, P.; Mitsiades, C.; Mitsiades, N.; Hayashi, T.; Munshi, N.; Dang, L.; Castro, A.; Palombella, V.; Adams, J.; Anderson, K. C. *J. Biol. Chem.* **2002**, *277*, 16639−16647.
(15) Shirley, R. B.; Kaddour-Djebbar, I.; Patel, D. M.; Lakshmikanthan, V.; Lewis, R. W.; Kumar, M. V. *Neoplasia* **2005**, *7*, 1104−1111.
(16) (a) Nesterenko, V.; Putt, K. S.; Hergenrother, P. J. *J. Am. Chem. Soc.* **2003**, *125*, 14672−14673. (b) Dothager, R. S.; Putt, K. S.; Allen, B. J.; Leslie, B. J.; Nesterenko, V.; Hergenrother, P. J. *J. Am. Chem. Soc.* **2005**, *127*, 8686−8696.

Scheme 1. Synthesis of the *trans*-Imidazolines[a]

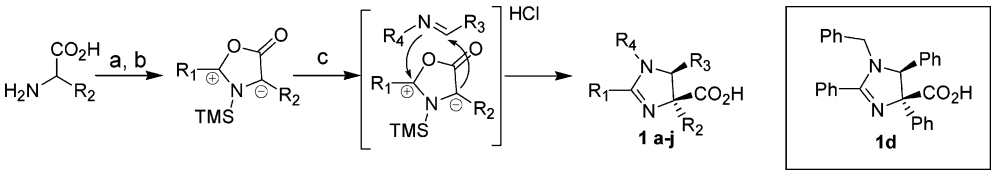

[a] (a) Acid chloride, NaOH (aq), Et_2O, overnight; (b) EDCI, CH_2Cl_2, 2 h, room temperature, 70−76% overall; (c) TMSCl, imine, CH_2Cl_2, reflux 4 h, room temperature overnight, 65−76%, (structures and activities of **1a**−**j**, Supporting Information Figure 1).

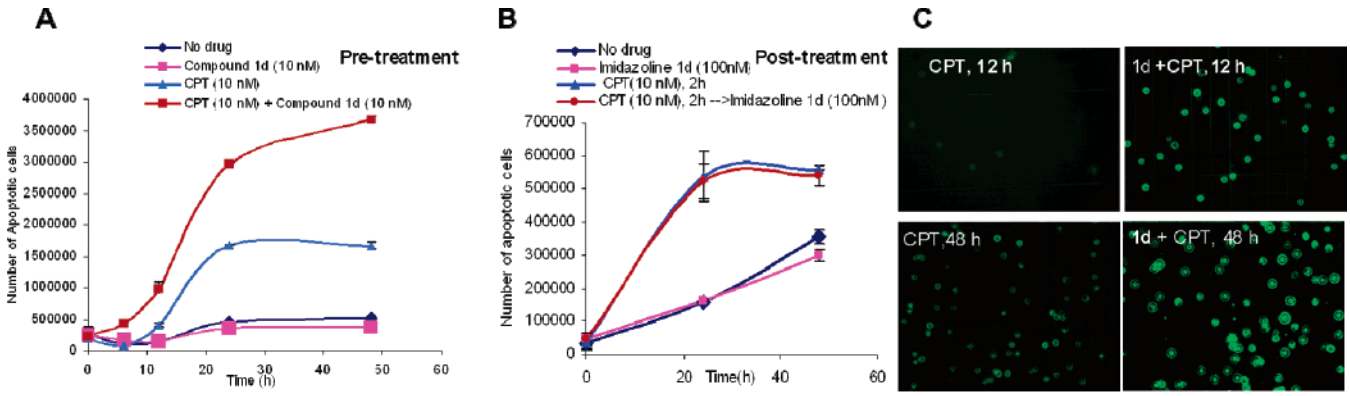

Figure 1. (A) Pretreated with the imidazoline **1d**. Caspase 3/7 activity in CEM cells treated with no drug control, imidazoline **1d** (10 nM), CPT (10 nM), and the combination of imidazoline **1d** (10 nM) followed by CPT (10 nM) after 0.5 h. (B) Post-treated with the imidazoline **1d**. Caspase 3/7 activity in CEM cells treated with no drug control, imidazoline **1d** (10 nM), CPT (10 nM), and the combination of CPT (10 nM) followed by imidazoline **1d** (10 nM) after 2 h. (C) Top left, CPT (10 nM), 12 h treatment; top right, combination pretreatment with **1d**, 12 h; bottom left, CPT (10 nM), 48 h; bottom right, combination pretreatment with **1d**, 48 h. All treatments stained with YoPro-1 and visualized using fluorescence microscopy.

Pioneering studies by Baldwin et al. demonstrated the control of inducible chemoresistance through inhibition of NF-κB via the incorporation of a mutated form of I-κBα, a natural inhibitor of NF-κB.[11,17] Piette et al. showed that the overexpression of mutated IκB-α regulated the cytotoxicity caused by camptothecin.[18] These studies illustrated the clinical potential of inhibition of NF-κB in combination chemotherapy. The most successful clinical example is the proteasome inhibitor bortezomib (PS-341), which may be used as a single agent or in combination regimens with classical anticancer agents providing a more than additive apoptotic response.[12,15,19,20]

Results and Discussion

Recently, we reported the imidazoline scaffold as a potent inhibitor of the NF-κB signaling pathway via the inhibition of the degradation of its inhibitory protein IκB.[21] Here, we report the ability of imidazoline **1d** to selectively sensitize cancer cells toward CPT and CDDP in CEM (acute leukemia), HT1080 (fibrosarcoma), and HeLa (cervical carcinoma) cells but not in the noncancerous SL89 (fibroblast) cell line. The imidazoline **1d** was identified as the most effective compound from a small library prepared via our previously reported TMSCl-mediated 1,3-dipolar cycloaddition of oxazolones and imines (Scheme 1).[22]

This library was evaluated for its ability to enhance CPT-induced apoptosis in CEM cells using a caspase-based Apo-One assay (Supporting Information Figure 1). Caspase activation plays a central role in the execution of apoptosis via the proteolytic cleavage of multiple protein substrates by caspase-3, -6, and -7.[23] NF-κB regulates programmed cell death via cross talk with the caspases.[8] Figure 1A illustrates the effect of the imidazoline **1d** on CEM cells when incubated with CPT over a 48-h time period. Enhancement of CPT-induced apoptosis in CEM cells was investigated at concentrations $\leq$10 nM CPT, which causes DNA aberrations but no significant apoptosis in leukemia cells.[17] Treatment of the cells with the imidazolines had no effect on the level of apoptosis (Figure 1A and Supporting Information Figure 3A), indicating that imidazolines do not exhibit significant cell cytotoxicity. Treatment with 10 nM CPT resulted in some cell death starting after 12 h. Combination treatment of the noncytotoxic imidazoline **1d** (10 nM) followed by CPT (10 nM) after 0.5 h resulted in complete apoptotic cell death after 48 h (Figure 1A, pretreatment). Interestingly, treatment of the cells with CPT (10 nM) followed by the addition of the imidazoline **1d** after 2 h did not show any enhancement of efficacy (Figure 1B, post-treatment). Consistent with the Apo-One assay, an increased cell permeability characterized by the increase in the fluorescence was observed when the Yo-Pro1 stained cell population was subjected to fluorescence microscopy (Figure 1C).

Post-Treatment with Imidazoline Does Not Potentiate CPT-Induced Apoptosis. Previously, we had shown that pretreatment of CEM cells with imidazoline **1d** inhibited the DNA binding activity of NF-κB, degradation of I-κBα, and

(17) Cusack, J. C., Jr.; Liu, R.; Baldwin, A. S., Jr. *Cancer Res.* **2000**, *60*, 2323−2330.
(18) Habraken, Y.; Piret, B.; Piette, J. *Biochem. Pharmacol.* **2001**, *62*, 603−616.
(19) An, J.; Sun, Y.; Fisher, M.; Rettig, M. B. *Leukemia* **2004**, *18*, 1699−1704.
(20) (a) Teicher, B. A.; Ara, G.; Herbst, R.; Palombella, V. J.; Adams, J. *Clin. Cancer Res.* **1999**, *5*, 2638−2645. (b) Orlowski, R. Z.; et al. *J. Clin. Oncol.* **2002**, *20*, 4420−4427. (c) Adams, J. *Curr. Opin. Chem. Biol.* **2002**, *6*, 493−500.
(21) Sharma, V.; Lansdell, T. A.; Peddibhotla, S.; Tepe, J. J. *Chem. Biol.* **2004**, *11*, 1689−1699.
(22) (a) Peddibhotla, S.; Tepe, J. J. *Synthesis* **2003**, *9*, 1433−1440. (b) Peddibhotla, S.; Jayakumar, S.; Tepe, J. J. *Org. Lett.* **2002**, *4*, 3533−3535.
(23) (a) Nicholson, D. W.; Thornberry, N. A. *Science* **2003**, *299*, 214−215. (b) Thornberry, N. A.; Lazebnik, Y. *Science* **1998**, *281*, 1312−1316. (c) Thornberry, N. A. *Chem. Biol.* **1998**, *5*, R97−103.

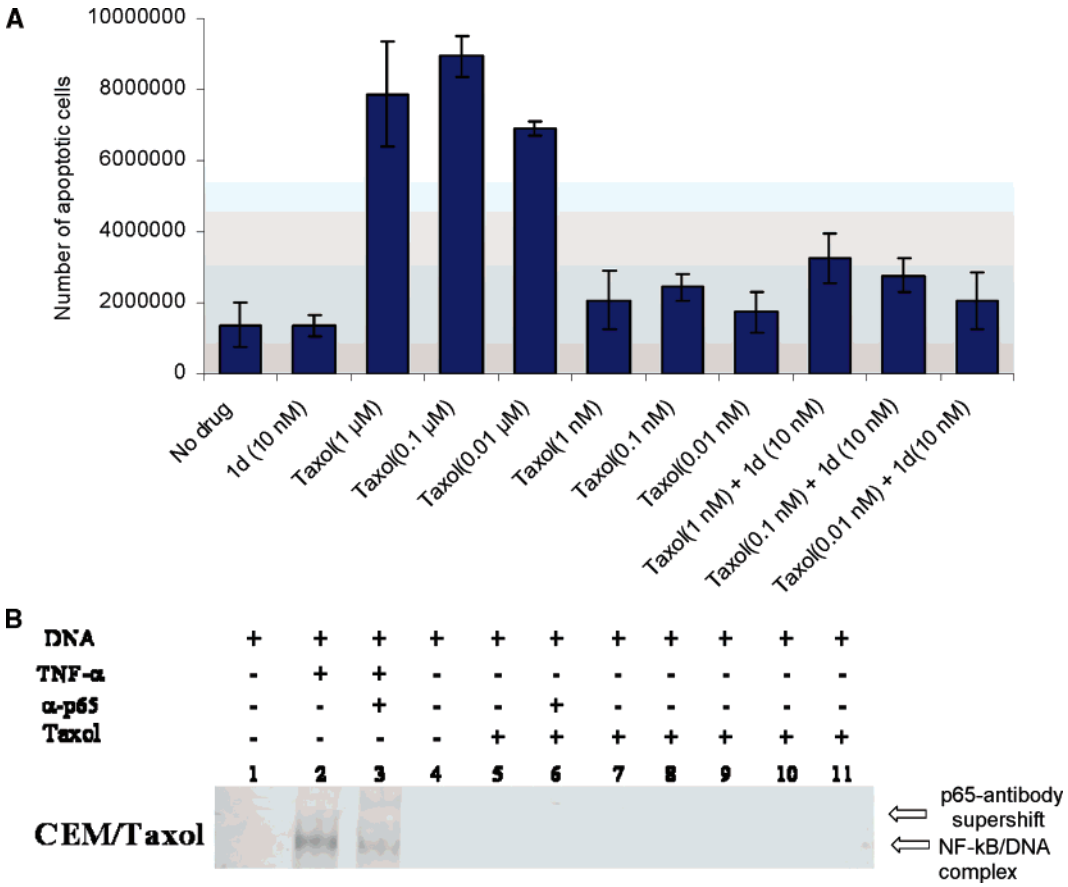

Figure 2. (A) Treatment of CEM cells with tubulin inhibitor Taxol. (B) EMSA of NF-κB activation in CEM cells by Taxol. DNA = oligonucleotide with NF-κB binding domain; TNF-α = endogenous activator of NF-κB; α-p65 = specific antibody for p65 unit of NF-κB; Taxol = chemotherapeutic agent.

transcriptional activity of NF-κB induced by CPT.[21] To further evaluate the relationship between the NF-κB signaling events and apoptosis induction by CPT, we determined the effect of pre- and post-treatment with imidazoline on CPT-induced apoptosis in CEM cells. Figure 1A (and Supporting Information Figure 3B) demonstrates that pretreatment of the cells with imidazoline **1d** significantly enhances apoptosis, whereas addition of the imidazoline 2 h after CPT treatment (Figure 1B) does not affect the induction of apoptosis (for both washed and continuous exposure, see Supporting Information Figure 3C). This differential effect of pre- or post-treatment with **1d** indicates that the pro-survival activation of NF-κB by CPT is likely to precede the apoptotic signaling in CEM cells.

Potentiation by the Imidazoline Scaffold Requires DNA Damage. We investigated whether imidazoline **1d** could potentiate drug-mediated cell death by various anticancer agents including taxol, vincristine, camptothecin, and cisplatin. In CEM cells, agents that induced DNA damage (cisplatin and camptothecin) consistently showed a strong enhancement of apoptosis on pretreatment with imidazoline. However, the imidazoline **1d** failed to significantly enhance tubulin inhibitors such as taxol (Figure 2A) and vincristine (Supporting Information Figure 4A) in CEM cells. Further investigation revealed that while taxol did not activate NF-κB in CEM cells, CPT activated NF-κB in a dose-dependent manner (Figures 2B and 4A). Activation of the NF-κB signaling cascade requires an intact nucleus and topoisomerase-1-mediated nuclear damage in CEM cells.[24] This suggests that the drug-induced apoptotic and anti-apoptotic signaling pathways related to DNA damage are crucial to the enhancement of efficacy by noncytotoxic imidazoline **1d**. This is in contrast to proteasome inhibitor bortezomib, which inhibits the NF-κB pathway and potentiates the effect of tubulin inhibitor taxol as well as DNA damaging agents, doxorubicin and cisplatin.[13,19]

Selective Potentiation of Drug-Mediated Apoptosis Induced by Imidazolines in Cancer Cells. The effect of imidazoline **1d** on cancer cells CEM, HT1080, HeLa, and noncancerous fibroblast cells (SL89) was quantified by calculating the concentration at which CPT and CDDP induced 95% apoptosis (CC_{95}) with and without pretreatment of the cells with imidazoline **1d** (100 nM for 0.5 h, CC_{95} combination). Table 1 clearly indicates that only the cancerous cell lines exhibited strong enhancement of apoptosis.

The CC_{95} values of both CPT and CDDP dropped drastically (up to 74-fold) upon pretreatment of cancerous cells with the imidazoline (Table 1 and Figure 3A). No increase in apoptosis was seen in the noncancerous fibroblasts (SL89) upon pretreatment with the noncytotoxic imidazoline **1d** (Table 1 and Figure 3B).

Correlation between Potentiation and NF-κB Activation. Our data indicate that sensitization of cells to chemotherapeutic agents using imidazoline **1d** exhibits a strong correlation with NF-κB activation. For example, CEM cells showed only moderate activation of NF-κB by CDDP (≥ 3 μM, Figure 4B) resulting in moderate fold enhancement (14-fold) compared to

(24) Huang, T. T.; Wuerzberger-Davis, S. M.; Seufzer, B. J.; Shumway, S. D.; Kurama, T.; Boothman, D. A.; Miyamoto, S. *J. Biol. Chem.* **2000**, *275*, 9501−9509.

Table 1. Cancer Cell Specific Enhancement of Efficacy[a]

cell line	drug	CC_{95}	CC_{95} combination	fold enhancement
CEM	CPT	44 nM	0.6 nM	74
CEM	CDDP	15 μM	1.1 μM	14
HT1080	CPT	86 μM	6.7 μM	13
HT1080	CDDP	1.48 μM	0.06 μM	24
HeLa	CPT	53 μM	5.2 μM	10
HeLa	CDDP	0.3 μM	0.06 μM	5
SL89	CPT	15 μM	16 μM	1
SL89	CDDP	0.5 μM	0.6 μM	1

[a] Data reported as an average of two independent experiments after 48 h of drug exposure. The imidazoline itself induced no significant levels of apoptosis (tested up to 10 μM). CPT = camptothecin, CDDP = cisplatin.

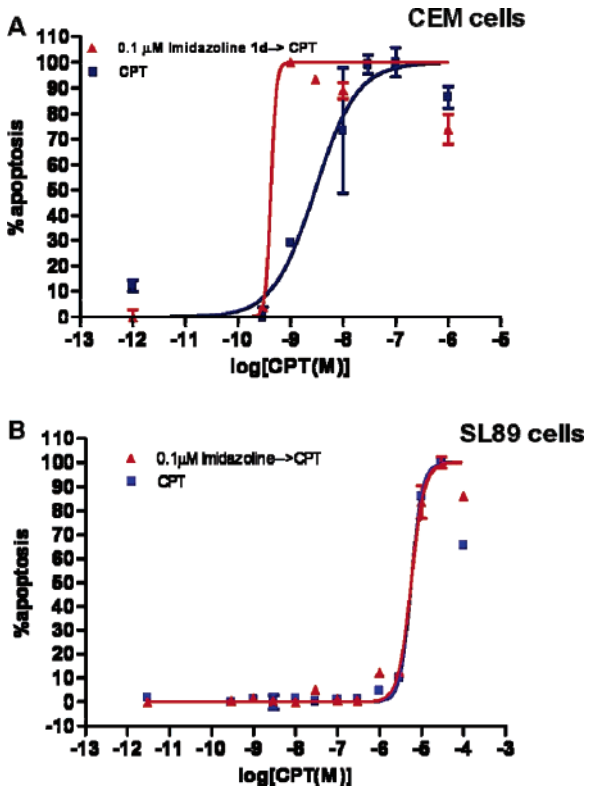

Figure 3. (A) CC_{95} comparison of CPT with and without imidazoline **1d** in CEM leukemia cells. (B) CC_{95} of CPT with and without imidazoline **1d** in noncancerous fibroblast cells. Data reported as an average of two independent experiments after 48 h of drug exposure.

the strong activation (≥0.01 μM, Figure 4A) and enhancement (74-fold) with CPT. This observation was noticeable across the panel of cell lines (Figure 4 and Table 1), in particular SL89 cells, which showed no enhancement with the imidazoline treatment (Figure 3B, Table 1) and were completely insensitive to NF-κB activation when treated with varying concentrations of either CPT, CDDP, or TNF-α (Figure 5).

This observation was further supported by the NF-κB driven transcription studied via a luciferase-based reporter assay in HeLa and SL89 cells. Both TNF-α as well as CPT activated NF-κB and enhanced NF-κB-based transcription in HeLa cells (Figure 6). SL89 cells were devoid of any significant NF-κB transcriptional activity (Figure 6), correlating well with the inability to show potentiation of DNA damage in the presence of imidazoline **1d**. However, it should be noted that even though the imidazoline is a potent modulator of the NF-κB signaling pathway via the inhibition of I-κB degradation, it is not yet known if NF-κB is the primary target of the imidazoline.

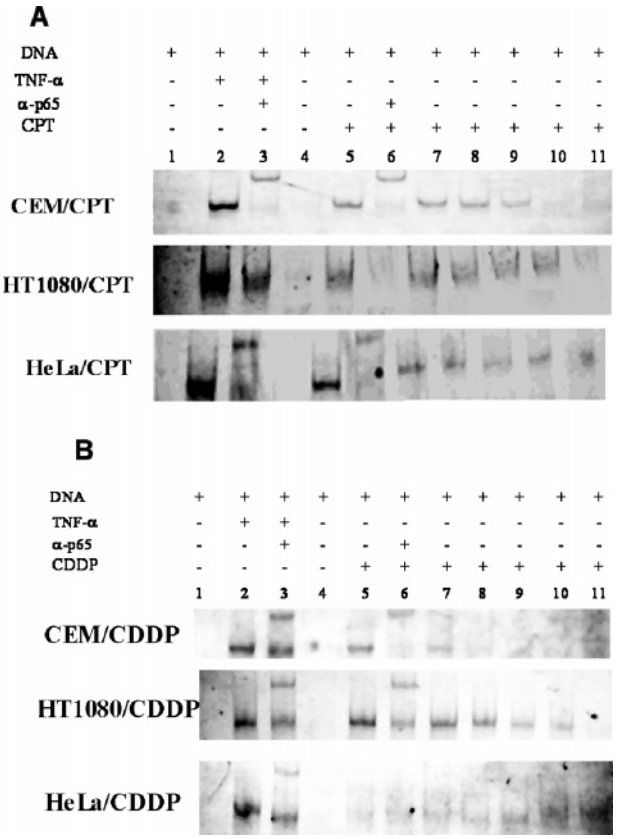

Figure 4. (A) EMSA for NF-κB−DNA binding in CEM, HT1080, and HeLa cells activated with various concentrations of CPT (lanes 5, 7−11: 10 μM, 1 μM, 0.1 μM, 0.01 μM, 1 nM, 0.1 nM). TNF-α was used as a positive control (lane 2), and CPT was used as a positive control (lane 5). A p65-specific antibody (α-p65) was used in lane 3 (TNF-α activation) and lane 6 (10 μM CPT activation) as a positive control. (B) EMSA for NF-κB−DNA binding in CEM, HT1080, and HeLa cells activated with various concentrations of CDDP (lanes 5, 7−11: 10 μM, 3 μM, 1 μM, 0.3 μM, 0.1 μM, and 0.03 μM). TNF-α was used as a positive control (lane 2), and CDDP was used as a positive control (lane 5). A p65-specific antibody (α-p65) was used in lane 3 (TNF-α activation) and lane 6 (10 μM CDDP activation) as a positive control.

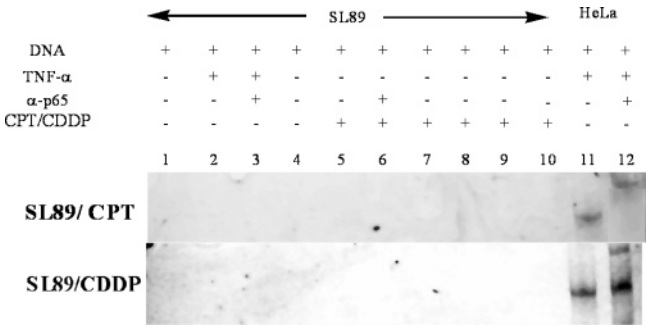

Figure 5. EMSA for NF-κB−DNA binding in SL89 cells. Cells were activated with TNF-α and CPT (10 μM, 1 μM, 0.1 μM, 0.01 μM, 1 nM) and CDDP (10 μM, 3 μM, 1 μM, 0.3 μM, and 0.1 μM). Hela cells activated with TNF-α were used as a positive control. The supershift with antibody specific for the p65 unit is shown in lane 12.

Chemical Resolution of 1d and Biological Activity of Enantiomers 2 and 3. Racemic **1d** was chemically resolved using an EDCI-mediated esterification with *R*-(+)-1-phenylethanol yielding two diastereomeric esters, which on hydrolysis afforded the (*S*,*S*) enantiomer **2** and (*R*,*R*) enantiomer **3** in overall 44% yield (Scheme 2). The enantiomers were crystallized, and their absolute configuration was determined by X-ray crystallography (Scheme 2).

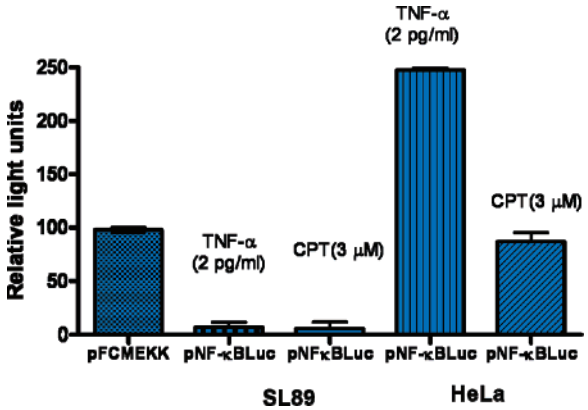

Figure 6. SL89 cells do not show NF-κB-mediated transcriptional activity with either TNF-α or CPT. pFCMEKK causes constitutive activation of NF-κB. pCIS-CK does not contain the enhancer element for NF-κB and serves as a negative control. TNF-α and CPT are known to activate NF-κB in a variety of cell lines.

The diastereomeric esters and the enantiomers **2** and **3** were tested for enhancement of apoptosis for a period of 48 h with CPT (Figure 7A). None of the compounds induced any significant cell death over 48 h; however, the (*R*,*R*) enantiomer **3** potentiated the apoptotic effect of CPT (CC_{95} combination = 0.53 nM, 83-fold enhancement) nearly 5 times more than the (*S*,*S*) enantiomer **2** (CC_{95} combination = 2.4 nM, 18-fold enhancement). The esters did not show a strong enhancement of apoptosis as determined by the caspase-based Apo-One assay (data not shown).

FACS Analysis. Apoptosis is a complex cellular mechanism involving characteristic changes within the nucleus, loss of mitochondrial function, membrane blebbing, etc.[1] CEM cells were treated with **1d**, **2**, and **3** for 30 min, followed by treatment with 0.01 μM CPT for 12 h and 48 h. At the desired time points, cells were harvested, stained, and sorted. As confirmed by the flow cytometry experiments, compounds **1d**, **2**, and **3** did not induce apoptosis themselves (Figure 7B, top panel), but enhanced apoptosis in combination with CPT (Figure 7B, bottom panel).

Conclusion

Conventional chemotherapy suffers a compromised clinical efficacy due to the induction of anti-apoptotic factors, concurrent with the desired induction of programmed cell death. The imidazoline **1d** is the lead compound from a novel class of nontoxic small molecules that enhance the efficacy of the DNA damaging agents. This is postulated to proceed via the inhibition of the pro-survival signaling pathways, such as NF-κB, in a highly cell-specific manner. In particular, imidazoline **1d** selectively sensitized cancer cells to genotoxic stress at low nanomolar concentrations. No such effect was seen in noncancerous fibroblasts. These studies indicate the potential of small-molecule NF-κB inhibitors to sensitize tumor cells toward classical anticancer agents in order to enhance the overall efficacy of anticancer treatment. Work toward identifying the target, detailed mechanism of action, and clinical potential of these agents is currently under investigation in our laboratories.

Experimental Section

Cell Culture. CEM cells ((CCRF-CEM); American Type Culture Collection, Rockville, MD) were grown in RPMI-1640 media (Gibco-BRL, Rockville, MD) supplemented with 10% fetal bovine serum, penicillin (614 ng/mL), streptomycin (10 μg/mL), and HEPES buffer, pH 7.2 at 37 °C, 5% CO_2. HT1080 and Hela cells were cultured in DMEM supplemented with 10% fetal bovine serum, penicillin (614 ng/mL), streptomycin (10 μg/mL), and HEPES buffer, pH 7.2 at 37 °C, 5% CO_2. SL89 cells were cultured in MEM supplemented with 10% fetal bovine serum, penicillin (614 ng/mL), and streptomycin (10 μg/mL) at 37 °C, 5% CO_2.

Scheme 2. Chemical Resolution of **1d** and X-ray Crystal Structures of **2** (*S*,*S*) and **3** (*R*,*R*)[a]

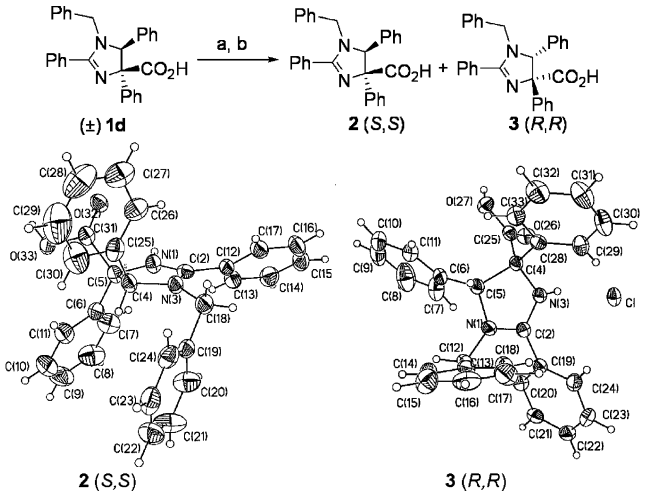

[a] (a) (*R*)-Phenylethanol, EDCI, DMAP, CH_2Cl_2; (b) 2 N NaOH/EtOH, reflux, 6 h, then HCl, 44% overall.

Optimization of Concentrations of Chemotherapeutic Agents for Apoptosis. Cells were cultured as described above. DMSO was used as the vector for all drugs and added in the control experiments. Cell cultures were treated with various concentrations of the camptothecin or cisplatin and allowed to incubate at 37 °C, 5% CO_2. At time points 0, 6, 12, 24, and 48 h, an aliquot of the cell culture was transferred to a 96-well plate and mixed with an equal volume of Apo-ONE Homogeneous Caspase-3/7 assay reagent (Promega Corporation). The contents of the plate were gently mixed and allowed to incubate for 30 min at room temperature. The fluorescence of each well was then measured on a Molecular Imager FXPro at 532 nm. All reported data is the average of two independent experiments unless otherwise indicated.

Enhancement of Apoptosis. CEM cells (CCRF-CEM) were cultured as described above. Cell cultures were treated with 0.1 μM, 0.01 μM, or 1 nM of the imidazoline **1d** and allowed to incubate at 37 °C, 5% CO_2 atmosphere for 30 min. Camptothecin was added at concentrations 50 μM, 1 μM, 0.3 μM, 0.1 μM, 0.03 μM, 0.01 μM, 3 nM, 1 nM, or 0.3 nM and further incubated. An aliquot was transferred to a 96-well plate at various time points 0, 6, 12, 24, and 48 h and mixed with an equal volume of Apo-ONE Homogeneous Caspase-3/7 assay (Promega Corporation) reagent. The contents of the plate were gently mixed and allowed to incubate for 1 h. The fluorescence of each well was then measured on a Molecular Imager FX Pro at 532 nm. All reported data is the average of two independent experiments unless otherwise indicated. The data were then analyzed using GraphPad prism 4.0, and CC_{95} values were calculated. Data were normalized between maximum and minimum cell death relative to the respective control sets.

EMSA Assay for NF-κB−DNA Binding. CEM cells were cultured as described above. Cells (1.6×10^6 cells/mL) were treated with TNF-α (0.4 pg) or camptothecin (Sigma-Aldrich) (10 μM, 1 μM, 0.1 μM, 0.01 μM, 1 nM, 0.1 nM) or CDDP (100 μM, 30 μM, 10 μM, 3 μM, 1 μM, 0.3 μM, 0.1 μM) at 37 °C and 5% CO_2 for 25 min or 2 h, respectively. SL89 cells were cultured as described above. Cells at 70% confluence were treated with TNF-α (0.4 pg) or camptothecin (Sigma-Aldrich) (10 μM, 1 μM, 0.1 μM, 0.01 μM, 1 nM) or CDDP (10 μM, 3 μM, 1 μM, 0.3 μM, 0.1 μM) at 37 °C and 5% CO_2 for 25 min or 2 h,

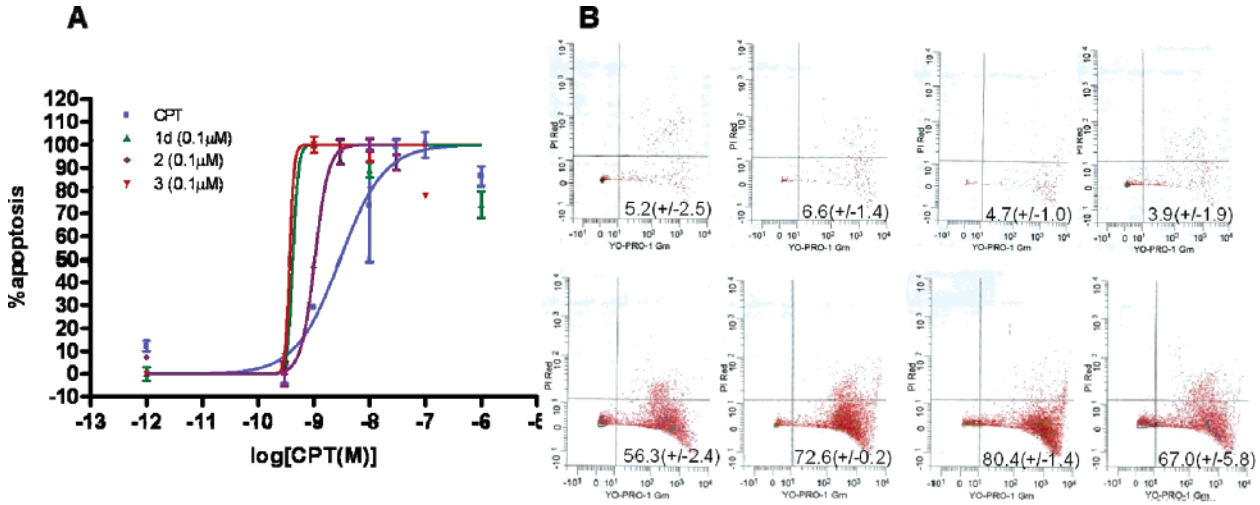

Figure 7. (A) Caspase 3/7 activity measured in CEM cells. CC_{95} comparison for CPT in CEM leukemia cells in the presence and absence of racemic **1d** and the enantiomers **2** and **3**. Data reported as an average of two separate experiments. (B) FACS analysis (top) cells alone, racemic **1d** (0.1 μM), **3** (0.1 μM), **2** (0.1 μM); (bottom) CPT (0.01 μM), **1d** → CPT (0.01 μM), **3** → CPT (0.01 μM), **2** → CPT (0.01 μM). The lower right quadrant indicates the % apoptosis (±standard deviation) for the sample.

respectively. The cells were harvested by centrifugation and washed in ice-cold PBS, and the nuclear extracts were prepared as previously described.[21] The protein concentration of the extracts was determined according to the Bradford method (1976) with BioRad reagents. Nuclear extracts (20 μg total protein) were incubated for 20 min at room temperature with a double-stranded Cy3-labeled NF-κB consensus oligonucleotide, 5′-AGTTGAGGGGACTTTC CCAGGC-3′ (0.16 pmol). The binding mixture (25 μL) contained 10 mM HEPES−NaOH, pH 7.9, 4 mM tris-HCl, pH 7.9, 6.0 mM KCl, 1 mM EDTA, 1 mM DTT, 10% glycerol, 0.3 mg/mL bovine serum albumin, and 1 μg of poly (dI.dC). The mixture was loaded on a 4% polyacrylamide gel prepared in 1X trisborate/EDTA buffer and was electrophoresed at 200 V for 20 min. After electrophoresis, the gel was analyzed using a phosphorimager (Biorad FX plus) for detection of the NF-κB−DNA binding.

NF-κB-Mediated Transcription in HeLa (Cervical Carcinoma) and SL89 (Noncancerous Fibroblast) Cells. Transient transfections were performed using lipofectamine 2000. Briefly, 0.8 μg of plasmid DNA was combined with lipofectamine 2000 (Invitrogen) (1.5 μL). The mixture was incubated at room temperature for 20 min and mixed with the cells without serum. Cells were transfected for 5 h at 37 °C in 5% CO_2. Cells were allowed to grow in complete medium for 15 h in 5% CO_2. Cells were then treated with TNF-α (10 ng/μL) or camptothecin (3 μM) for 5 h or 10.5 h, respectively. Cells were washed with 1 × PBS. Washed cells were assayed for luciferase production using the manufacturer's protocol for both luciferase as well as renilla luciferase (co-reporter) using the Dual-Glo reporter assay (Promega). The results were read on a Veritas microplate luminometer (Turner Biosystems, CA) as relative light units. Values from the luciferase activity were normalized to those with renilla luciferase.

FACS Analysis. CEM cells were cultured as described above. Cell cultures were treated with 0.1 μM imidazoline **1d**, **2**, or **3** and allowed to incubate at 37 °C, 5% CO_2 atmosphere for 30 min. Camptothecin was added at 0.01 μM and further incubated for 12 and 48 h to mark early and late apoptotic events. Cells were then harvested and washed in 1 × PBS. Cells were stained with Yo-Pro1 and propidium iodide to mark the apoptotic cells. These were then analyzed on a BD Biosciences Vantage SE (San Jose, CA) flow cytometer using a 530/30 band-pass filter for Yo-Pro1 and 660/20 (band-pass filter) for PI, respectively.

Fluorescence Microscopy. CEM cells (CCRF-CEM) were cultured as described above. Cell cultures were treated with 0.1 μM imidazoline **1d**, **2**, or **3** and allowed to incubate at 37 °C, 5% CO_2 atmosphere for 30 min. Camptothecin was added at 0.01 μM and further incubated for 12 and 48 h to mark early and late apoptotic events. Cells were then harvested, stained with Yo-Pro-1, and visualized under a fluorescence microscope Olympus CK2 using a BP480-550C filter.

Compound 1d. dl-(3*S*,4*S*)-1-Benzyl-2,4,5-triphenyl-4,5-dihydro-1*H*-imidazole-4-carboxylic Acid. A solution of benzaldehyde (0.6 g, 5.7 mmol) and benzylamine (0.61 g, 5.7 mmol) in dry dichloromethane (120 mL) was refluxed under nitrogen for 2 h. 2,4-Diphenyl-4*H*-oxazolin-5-one (1.35 g, 5.7 mmol) and chlorotrimethylsilane (0.8 g, 7.4 mmol) were added, and the mixture was refluxed under nitrogen for 6 h and then stirred overnight at room temperature. The product was purified by silica gel column chromatography with 1:5 ethanol/ethyl acetate to afford 2.1 g of the product in 65% yield as an off-white solid. Mp 153−155 °C dec. ^{1}H NMR (300 MHz) ($CDCl_3$): δ 3.8 (1H, d, J = 15.6 Hz), 4.62 (1H, d, J = 15.6 Hz), 4.98 (1H, s), 6.58 (2H, d, J = 8.1 Hz), 7.05−7.65 (16H, m), 7.9 (2H, d, J = 7.2 Hz); ^{13}C NMR (75 MHz) ($CDCl_3$): δ 48.3, 75.6, 79.1, 123.1, 125.7, 126.7, 127.3, 127.4, 127.9, 128.1, 128.2, 128.8, 128.9, 129, 129.3, 132.9, 133.8, 136, 143.1, 164.8, 168.1; IR (neat): 3400 cm^{-1} (very broad), 1738 cm^{-1}; HRMS (EI): calcd for $C_{29}H_{24}N_2O_2$ $[(M - H) - CO_2]^+$ 387.1526 and obsd $[(M - H) - CO_2]^+$ 387.1539.

Compounds 2 and 3. In a flame-dried flask, under nitrogen, a well-stirred suspension of 1-benzyl-2,4,5-triphenyl-4,5-dihydro-1*H*-imidazole-4-carboxylic acid (0.1 g, 0.18 mmol) in dry methylene chloride (20 mL) was maintained at 0 °C. To this mixture was added EDCI·HCl (36 mg, 0.18 mmol), followed by DMAP (22 mg, 0.18 mmol), and stirred for 20 min. (*R*)-(+)-1-phenylethanol (43.5 mg, 2 equiv, 0.36 mmol) was added, and the mixture was stirred overnight at room temperature. The reaction mixture was washed with 2 N HCl (2 × 20 mL), with saturated sodium bicarbonate (2 × 20 mL), and then with brine (20 mL). The organic layer was dried over sodium sulfate and evaporated under reduced pressure. The crude product was purified by column silica gel chromatography using 40% ether/hexane mixture. These were characterized and subjected to hydrolysis under reflux with 2 N NaOH/EtOH separately. The reaction mixtures were cooled and acidified to pH = 3 and extracted with $CHCl_3$. The organic layer was dried and evaporated in vacuo to obtain the two enantiomers in 44% yield.

***S,S,R*-1-Benzyl-2,4,5-triphenyl-4,5-dihydro-1*H*-imidazole-4-carboxylic Acid 1-Phenylethyl Ester:** $[\alpha]_D$ +19.45°, *c* 1, $CHCl_3$; ^{1}H NMR (300 MHz), $CDCl_3$: δ 0.873 (d, J = 6.6, 3H), 3.73 (d, J = 15 Hz, 1H), 4.56 (d, J = 15 Hz, 1H), 4.93 (s, 1H), 5.23 (q, J = 6.5, 1H), 6.73−7.72 (m, 25H); ^{13}C NMR (74.4 MHz) $CDCl_3$: 21.80, 48.53, 72.77, 73.26, 82.32, 125.73, 126.75, 127.23, 127.30, 127.38, 127.94, 128.26, 128.37, 128.54, 128.58, 128.74, 130.29, 130.34, 136.47, 137.69,

141.37, 143.58, 165.38, 169.79; IR($CHCl_3$): 3584.2, 3063.4, 3032.5, 2926.4, 2855.0, 1736.1, 1595.3, 1495.0, 1412.1, 1064.8 cm^{-1}; EIMS: m/z = 537.2 (M + H), 387.3 (M − COOCH(Me)Ph); HRMS (FAB+) ($C_{37}H_{33}O_2N_2$) (M + H) 537.2542; found, 537.2542.

***R,R,R*-1-Benzyl-2,4,5-triphenyl-4,5-dihydro-1*H*-imidazole-4-carboxylic Acid 1-Phenylethyl Ester.** $[\alpha]_D$ −7.77°, *c* 1, $CHCl_3$; ^1H NMR (300 MHz), $CDCl_3$: δ 1.205 (d, J = 6.6, 3H), 3.73 (d, J = 15 Hz, 1H), 4.56 (d, J = 15 Hz, 1H), 4.95 (s, 1H), 5.23 (q, J = 6.5, 1H), 6.80−7.81 (m, 25H); ^{13}C NMR (74.4 MHz) $CDCl_3$: 21.75, 48.50, 73.42, 73.49, 82.87, 126.01, 126.87, 127.14, 127.29, 127.35, 127.95, 127.99, 128.13, 128.20, 128.40, 128.57, 128.75, 130.23, 36.72, 137.28, 141.00, 143.95, 165.50, 169.94; IR($CHCl_3$): 3584.2, 3063.4, 3032.5, 2924.5, 2855.0, 1736.2, 1595.3, 1495.0, 1412.1, 1064.8 cm^{-1}; EIMS: m/z = 537.3(M + H), 387.3 (M − COOCH (Me) Ph) HRMS (FAB+) ($C_{37}H_{33}O_2N_2$) (M + H) 537.2542; found, 537.2542.

(4*S*,5*S*)-1-Benzyl-4, 5-dihydro-2,4,5-triphenyl-1*H*-imidazole-4-carboxylic Acid (2): Mp 148−149 °C dec. $[\alpha]_D$ −47.58°, *c* 1, $CHCl_3$; ^1H NMR (300 MHz), $CDCl_3$: δ 3.96 (d, J = 15 Hz, 1H), 4.81 (d, J = 15 Hz,1H), 5.05 (s, 1H), 6.61 (2H, d, J = 8.1 Hz), 7.09−7.92 (16H, m), 7.90 (2H, d, J = 7.2 Hz), 11.42 (s, 1H); ^{13}C NMR (74.4 MHz) $CDCl_3$: 49.37, 75.33, 76.06, 121.29, 125.93, 127.65, 129.24, 129.40, 129.42, 129.86, 130.02, 130.14, 130.76, 131.69, 131.82, 132.18, 134.62, 138.54, 166.69, 167.71; IR($CHCl_3$): 3584.2, 3063.4, 2924.5, 1743.9, 1558.9, 1456.4, 1253.9 cm^{-1}; EIMS: m/z = 387.3 (M − COOH) HRMS (FAB+) ($C_{29}H_{25}O_2N_2$) (M + H) 433.1916; found, 433.1914.

(4*R*,5*R*)-1-Benzyl-4,5-dihydro-2,4,5-triphenyl-1*H*-imidazole-4-carboxylic Acid (3·HCl): Mp 147−148 °C dec. $[\alpha]_D$ +47.87°, *c* 1, $CHCl_3$; mp 147−149 °C dec. ^1H NMR (300 MHz), $CDCl_3$: δ 4.02 (d, J = 15 Hz, 1H), 4.84 (d, J = 15 Hz, 1H), 5.09 (s, 1H), 6.61 (2H, d, J = 8.1 Hz), 7.12−7.77 (16H, m), 7.97 (2H, d, J = 7.2 Hz); ^{13}C NMR (74.4 MHz) $CDCl_3$: 48.76, 74.96, 77.03, 121.45, 125.90, 126.57, 127.15, 128.29, 128.48, 128.57, 128.81, 129.12, 129.39, 129.56, 129.65, 130.09, 132.47, 132.84, 133.01, 134.14, 139.96, 165.84, 168.34; IR($CHCl_3$): 3584.2, 3063.4, 2924.5, 1741.9, 1556.7, 1456.4, 1221.1 cm^{-1}; EIMS: m/z = 386.3 (M − COOH − H) HRMS (FAB+) ($C_{29}H_{25}O_2N_2$) (M + H) 433.1916; found, 433.1915. LRMS (FAB−) 35, 37.

Acknowledgment. We gratefully acknowledge the American Cancer Society for their financial support (Research Scholar Award, RSG-04-018-01-CDD). The authors also thank the MSU Foundation for financial support. We greatly acknowledge Dr. Rui Huang for carrying out the X-ray crystallography. V.S. gratefully acknowledges the College of Natural Science, MSU for The Graduate School Dissertation Fellowship during the course of preparation of this manuscript.

Supporting Information Available: Additional cell toxicity data, initial caspase-based screen, potentiation with CPT and CDDP in various cell lines, toxicity data with tubulin inhibitors, post-treatment with imidazoline, X-ray data tables and CIF files, ^1H and ^{13}C for all new compounds, and complete ref 20b. This material is available free of charge via the Internet at http://pubs.acs.org.

JA060273F